

## Supporting Information

### Differential Regulation of SIRT5 Activity by Reduced Nicotinic Acid Riboside (NARH)

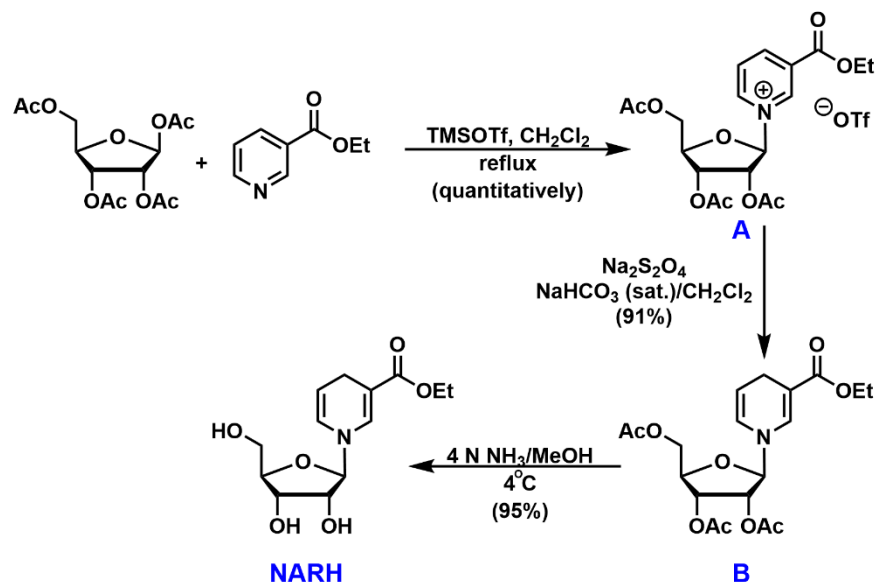
Abu Hamza<sup>‡</sup>, Dickson Donu<sup>‡</sup>, Emily Boyle<sup>‡</sup>, Rasajna Madhusudhana<sup>‡</sup>, Alyson Curry<sup>‡</sup>, Yana  
Cen<sup>‡,#,\*</sup>

<sup>‡</sup>*Department of Medicinal Chemistry, Virginia Commonwealth University, Richmond, VA 23219*

<sup>#</sup>*Center for Drug Discovery, Virginia Commonwealth University, Richmond, VA 23219*

\*Correspondence: [ceny2@vcu.edu](mailto:ceny2@vcu.edu), phone: 804-828-7405

## Synthesis of NARH



### Synthesis of Intermediate A

Intermediate **A** was synthesized as described previously.<sup>1, 2</sup>

### Synthesis of Intermediate B

In a round bottom flask flushed with argon, intermediate **A** (2.84 g, 5.08 mmol) was dissolved in 40 mL of  $\text{CH}_2\text{Cl}_2$ . To this solution was added 13 mL of saturated aqueous  $\text{NaHCO}_3$  solution, followed by solid sodium dithionite (ca. 85%; 4.27 g; 20.9 mmol) and 7 mL of water. The biphasic reaction mixture was stirred at room temperature for 4 h, and then brine (30 mL) and  $\text{CH}_2\text{Cl}_2$  (40 mL) were added. Yellow organic phase was separated, washed twice with brine, dried over  $\text{Na}_2\text{SO}_4$ , filtered and evaporated under reduced pressure to give a light yellow foam (intermediate **B**). The crude product was used for the next step without further purification.

### Synthesis of NARH

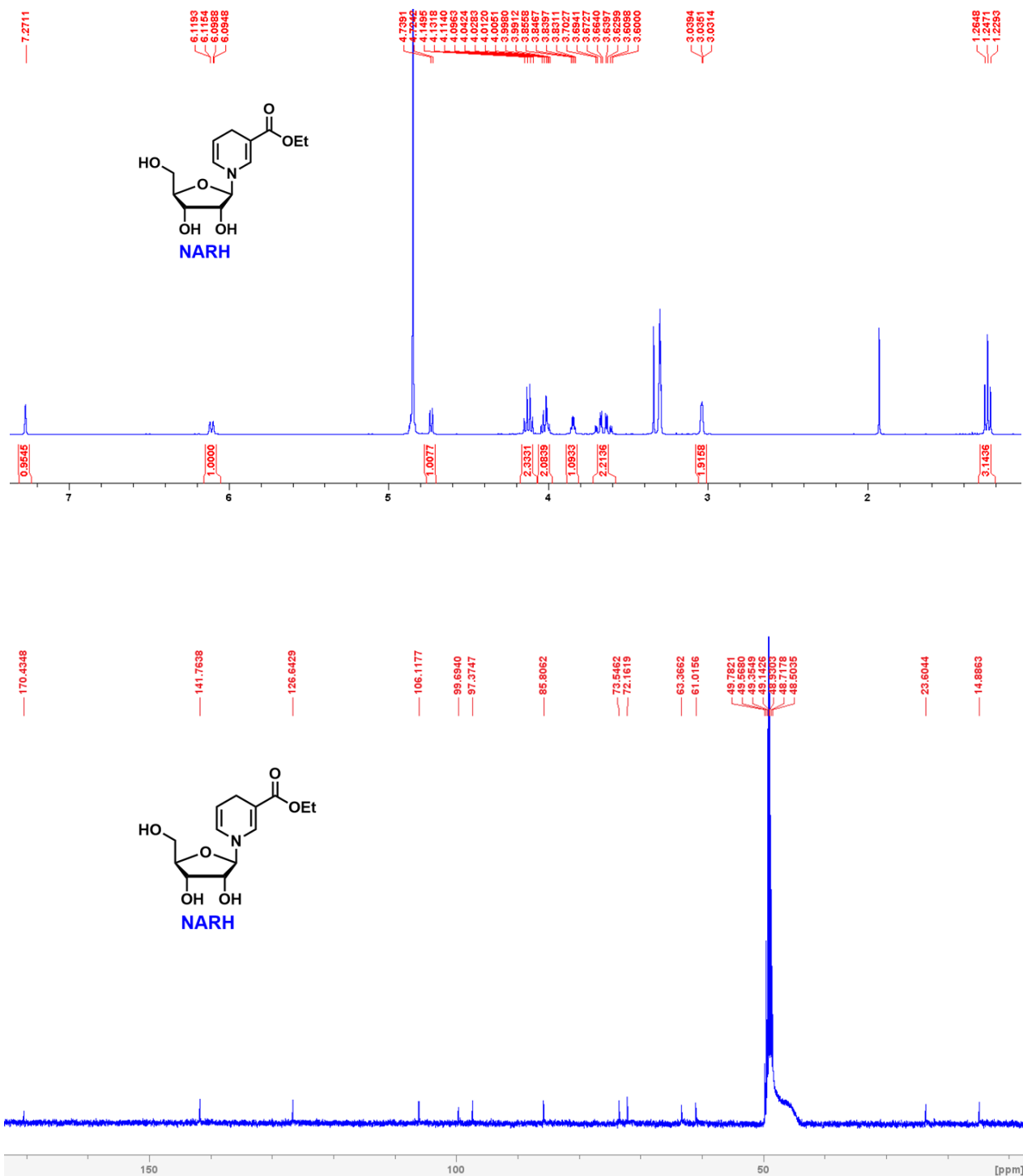
Intermediate **B** (1.90 g, 4.62 mmol) was dissolved in 15 mL of methanol and 20 mL of 7N  $\text{NH}_3$  in methanol at  $0^\circ\text{C}$ . The reaction was kept at  $4^\circ\text{C}$  for 16 h before solvent was removed under reduced pressure. The residue was dissolved in water and extracted with hexanes to remove

organic impurities. The water layer was concentrated and purified by silica gel column chromatography ( $\text{CH}_2\text{Cl}_2$  with 5%~10% methanol) to afford **NARH** (1.25 g, 4.37 mmol, 86% yield for two steps) as a pale yellow oil.  $^1\text{H}$  NMR ( $\text{CD}_3\text{OD}$ , 400 MHz)  $\delta$  (ppm): 1.25 (t,  $J = 7.1$  Hz, 3H), 3.04 (m, 2H), 3.61 (dd,  $J = 3.9, 12.0$  Hz, 1H), 3.68 (dd,  $J = 3.4, 12.0$  Hz, 1H), 3.84 (m, 1H), 4.00 (m, 2H), 4.12 (q,  $J = 7.1$  Hz, 2H), 4.73 (d,  $J = 6.0$  Hz, 1H), 6.10 (dd,  $J = 1.6, 8.2$  Hz, 1H), 7.27 (s, 1H);  $^{13}\text{C}$  NMR ( $\text{CD}_3\text{OD}$ , 100 MHz): 14.89, 23.60, 61.02, 63.37, 72.16, 73.55, 85.81, 97.37, 99.69, 106.12, 126.64, 141.76, 170.43; HRMS ( $m/z$ ): calculated for  $\text{C}_{13}\text{H}_{19}\text{NNaO}_6$  ( $\text{M}+\text{Na}$ ): 308.1105; found: 308.1114.

### Synthesis of MalAM-yne

MalAM-yne was synthesized as reported previously.<sup>3</sup>  $^1\text{H}$  NMR ( $\text{CDCl}_3$ , 400 MHz)  $\delta$  (ppm): 2.06 (t,  $J = 2.6$  Hz, 1H), 2.14 (s, 6H), 2.84 (dd,  $J = 2.7, 7.6$  Hz, 2H), 3.70 (t,  $J = 7.6$  Hz, 1H), 5.80 (d,  $J = 1.7$  Hz, 4H).

**Figure S1.** NMR and MS spectra of NARH.



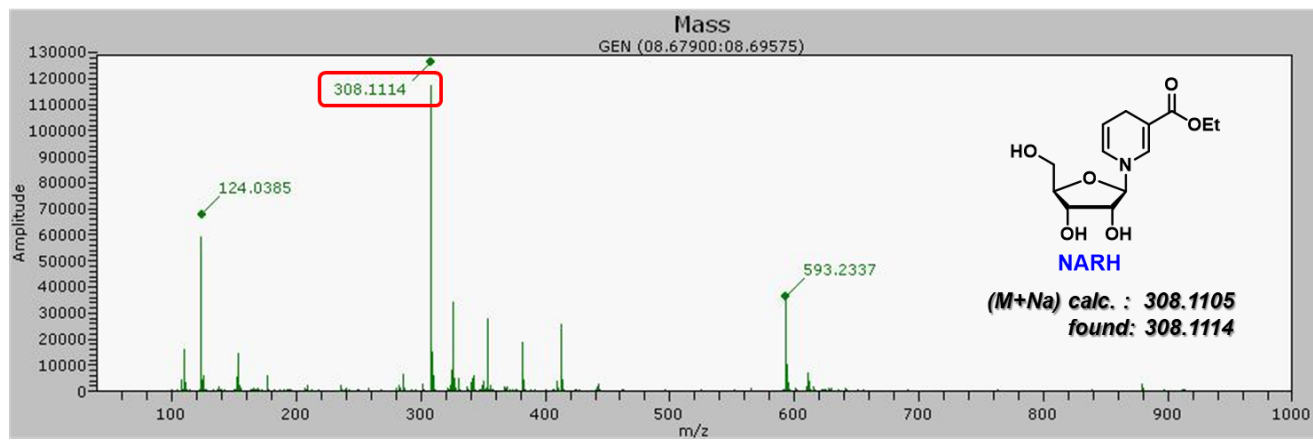


**Figure S2.**  $^1\text{H}$  NMR spectrum of MalAM-yne.

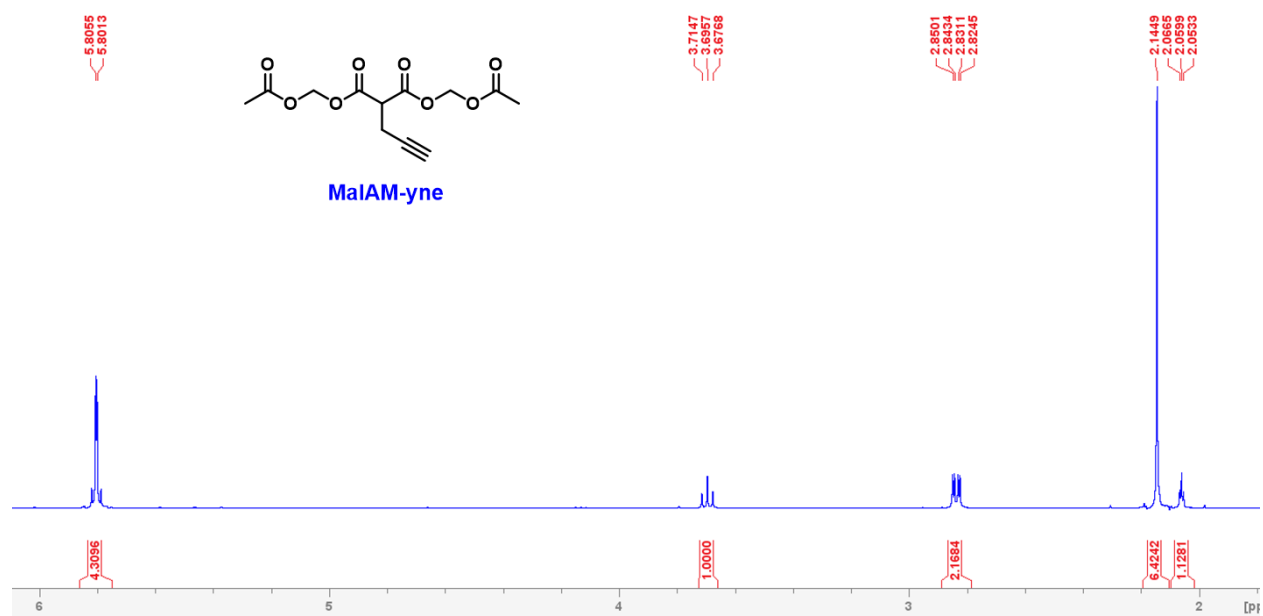
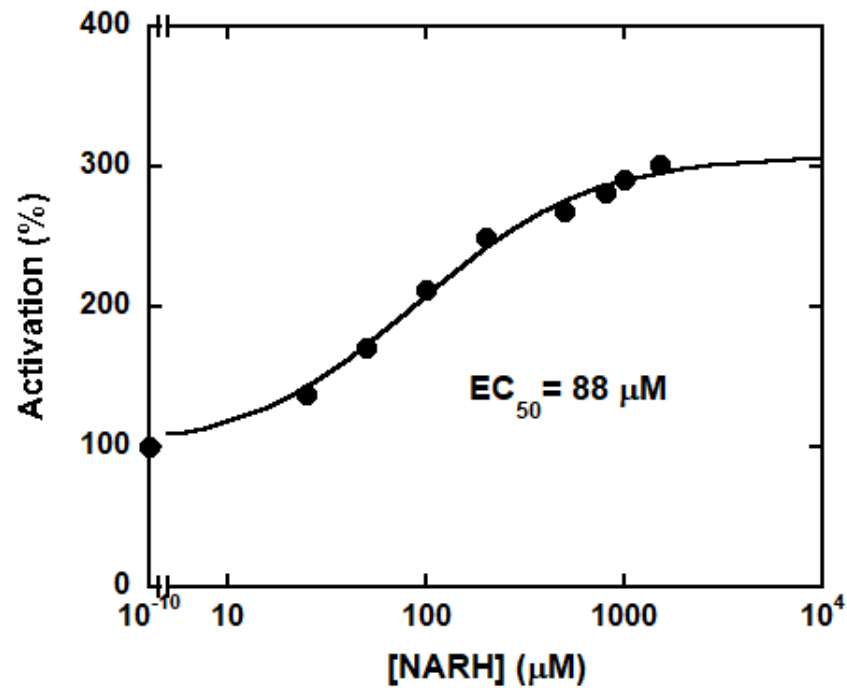
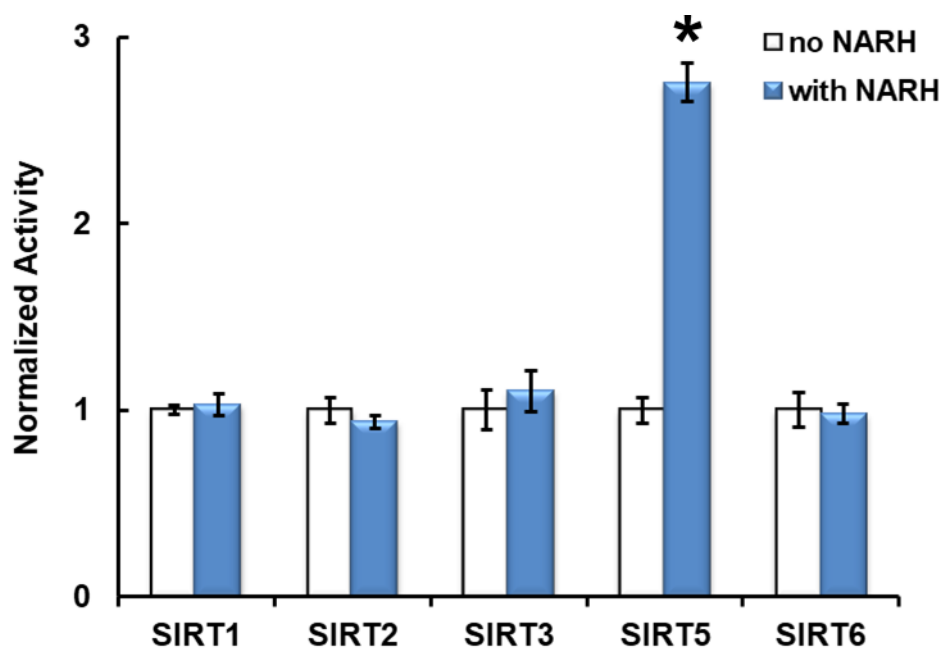


**Figure S3.** Dose-dependent activation of SIRT5 desuccinylation by NARH.



SIRT5 was incubated with  $\text{NAD}^+$ , H3K9Suc, and varying concentrations of NARH. The samples were then injected on an HPLC fitted to a Macherey-Nagel Nucleosil C18 column. Succinylated and desuccinylated peptides were resolved using a gradient of 10%–40% acetonitrile in 0.1% TFA. Chromatograms were analyzed at 215 nm. Reactions were quantified by integrating area of peaks corresponding to succinylated and desuccinylated peptides. The  $\text{EC}_{50}$  was determined to be  $88 \mu\text{M}$ .

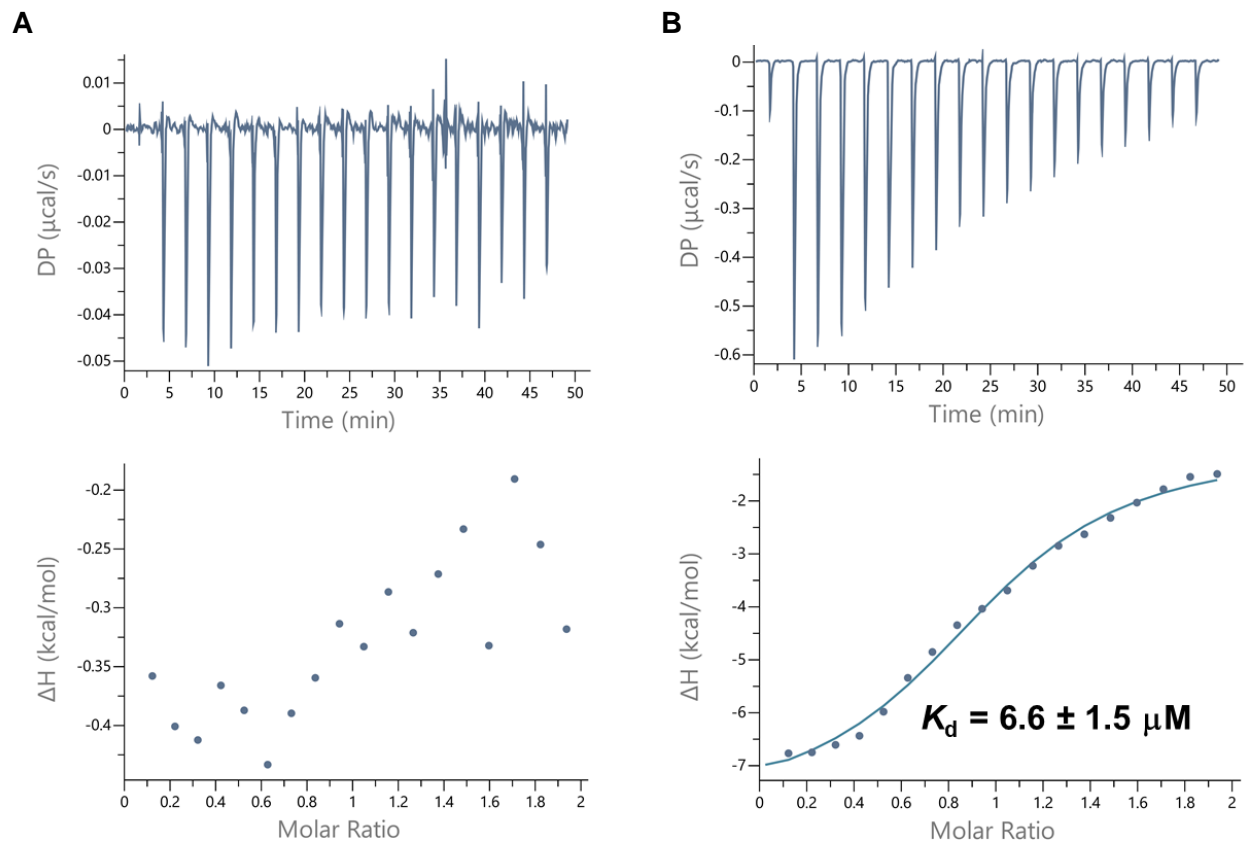
**Figure S4.** NARH activates SIRT5 selectively.



A typical reaction contained 800  $\mu\text{M}$   $\text{NAD}^+$ , 500  $\mu\text{M}$  peptide substrate (H3K9Ac for SIRT2, SIRT3 and SIRT6, p53K382Ac for SIRT1, and H3K9Suc for SIRT5), with or without 800  $\mu\text{M}$  NARH in 100 mM phosphate buffer pH 7.5. The reactions were initiated by the addition of 10  $\mu\text{M}$  of sirtuin and were incubated at 37  $^{\circ}\text{C}$  before being quenched by 8  $\mu\text{L}$  of 10% TFA. The incubation time was controlled so that the conversion of substrate was less than 15%. The samples were then injected on an HPLC fitted to a Macherey-Nagel Nucleosil C18 column. Acylated and deacylated peptides were resolved using a gradient of 10%–40% acetonitrile in 0.1% TFA. Chromatograms were analyzed at 215 nm. Reactions were quantified by integrating area of peaks corresponding to acylated and deacylated peptides. The data represents average of as least three independent experiments  $\pm$  S.D. Statistical significance was determined by a Student's t-test: \* $p < 0.01$ .

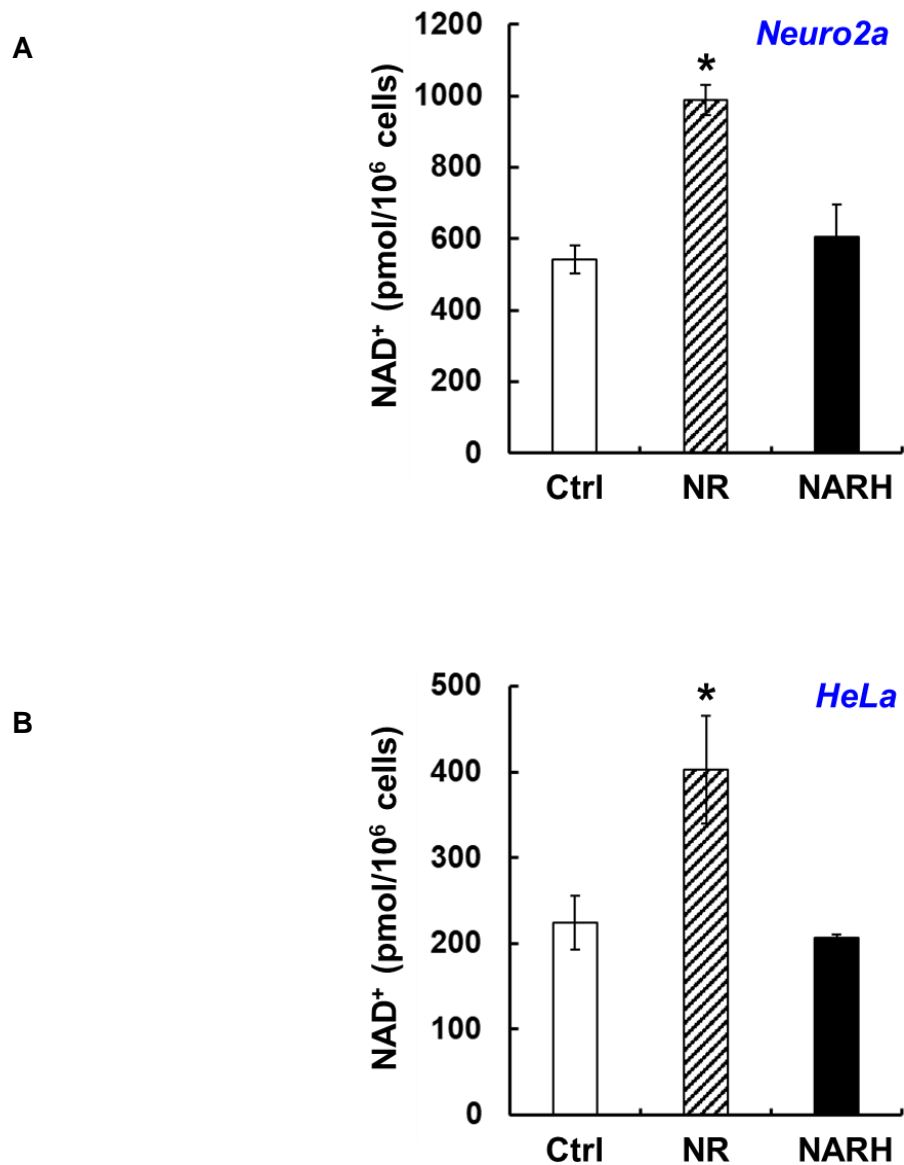


**Figure S5.** ITC studies.



Representative ITC traces of NAD<sup>+</sup> (500  $\mu\text{M}$ , A) or a mixture of NAD<sup>+</sup> and NARH (500  $\mu\text{M}$  each, B) titrated into SIRT5 (50  $\mu\text{M}$ ). The experimental details can be found in “Methods and Materials”.

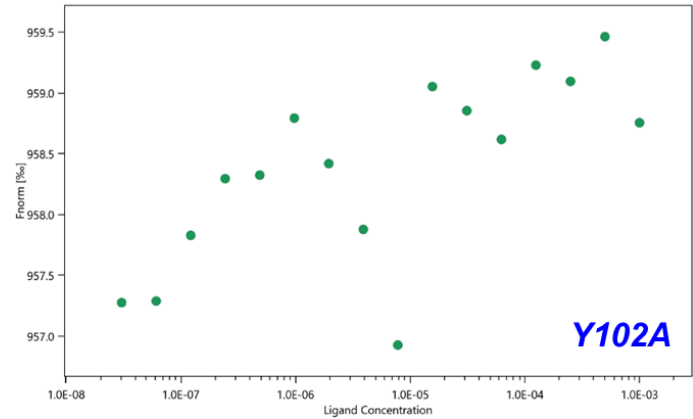
**Figure S6.** NARH treatment does not increase cellular NAD<sup>+</sup> levels.



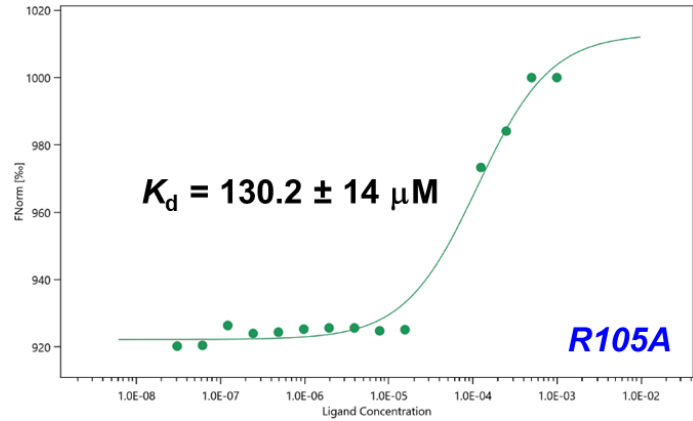
Intracellular NAD<sup>+</sup> levels in Neuro2a (A) and HeLa (B) cells. The cells were incubated with vehicle, 1 mM NR, or 1 mM NARH for 6 h. Subsequently, the intracellular NAD<sup>+</sup> concentrations were determined as described in “Methods and Materials”. The quantification data represents the average of three independent experiments  $\pm$  SD. Statistical significance was determined by a Student’s *t*-test: \**p* < 0.05 vs control.

**Figure S7.** MST measurements of SIRT5 mutant binding to NARH.

**A**



**B**



**C**

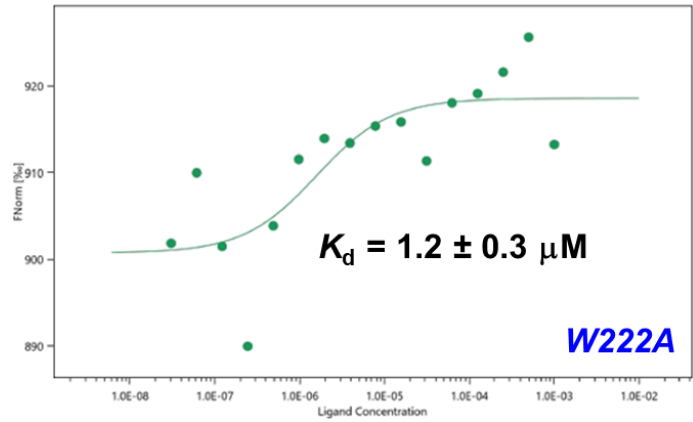
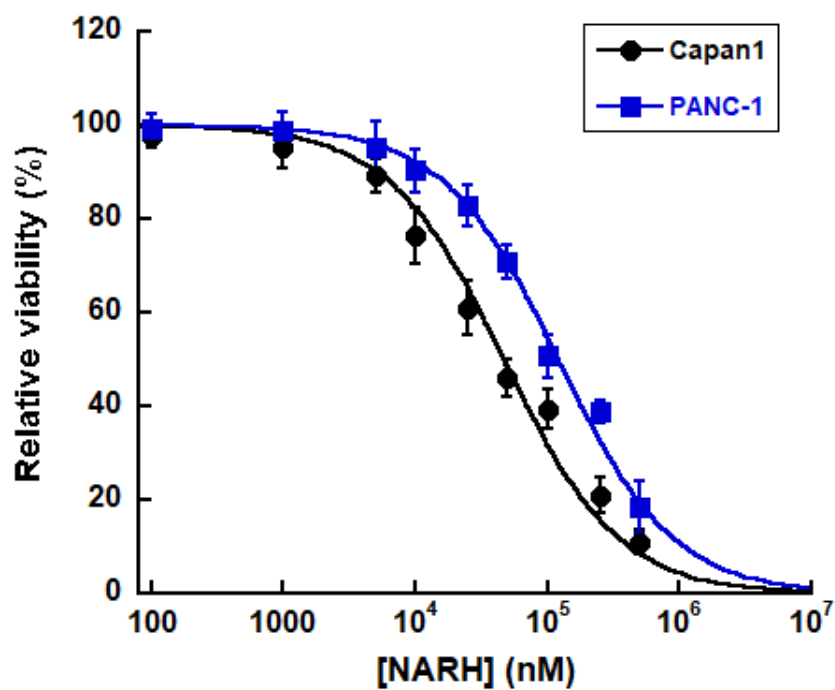
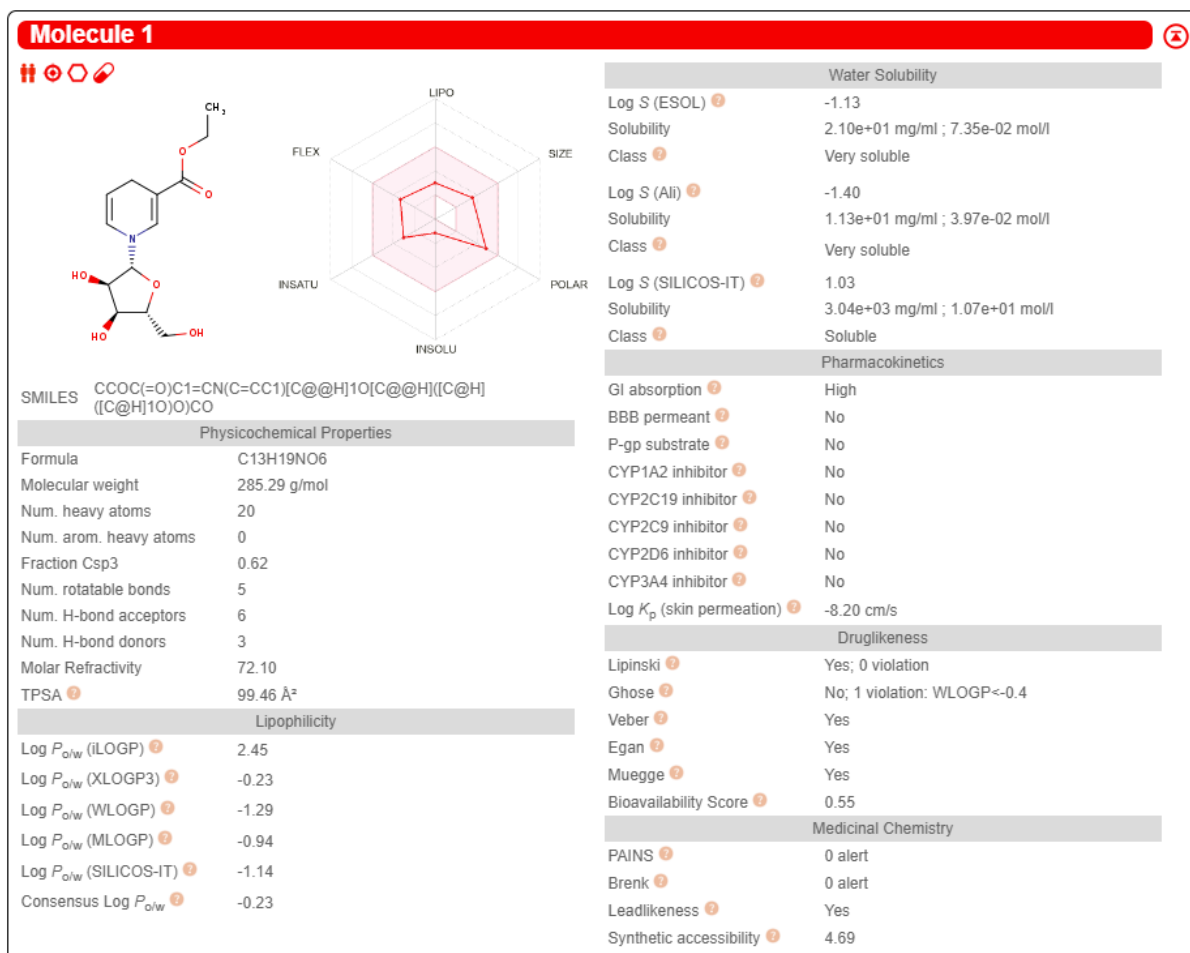


**Figure S8.** Cell viability of NARH-treated PDAC cells.



Cell viability was measured using the Cell Counting Kit-8 (MedChemExpress) following the manufacturer's instruction. The IC<sub>50</sub> values were  $46.7 \pm 3.5 \mu\text{M}$  and  $120.7 \pm 7.4 \mu\text{M}$  for Capan-1 and PANC-1 cells, respectively.

**Figure S9.** ADME prediction of NARH.



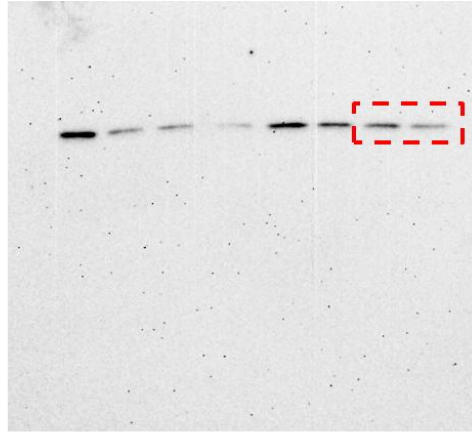
The physicochemical, ADME, and drug-likeness parameters of NARH were computed using the SwissADME online program (<http://www.swissadme.ch>).<sup>4</sup>

## Raw Data Files for Gels and Blots

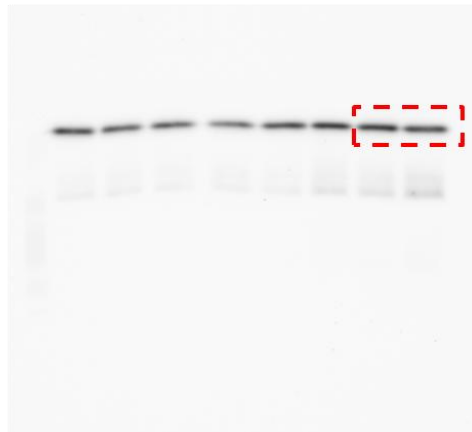
**Figure 3.** Activation of SIRT5 by NARH on physiological substrates.

**A**

**CPS1Suc**



**CPS1**



**B**

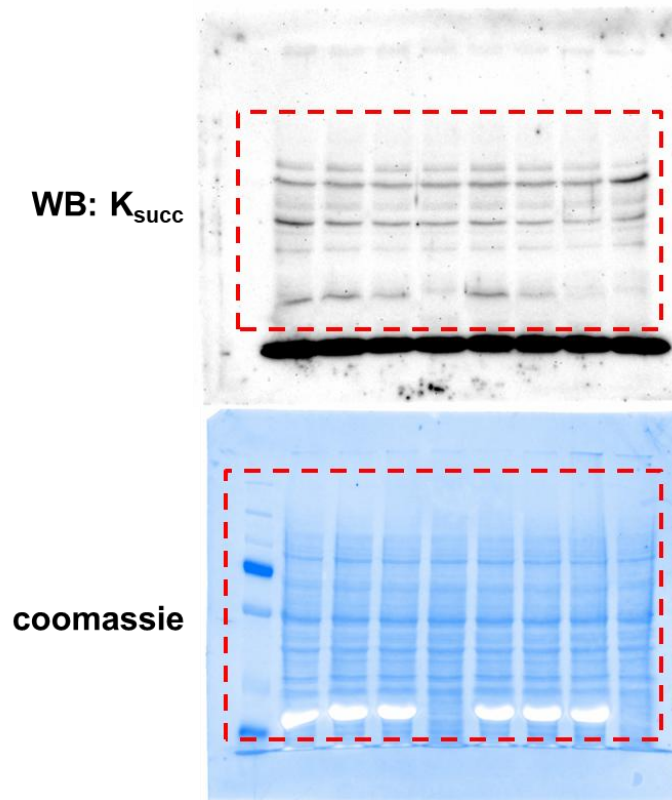
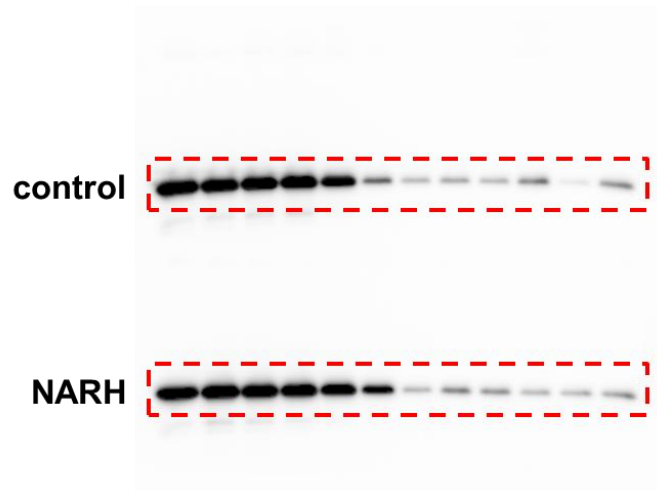
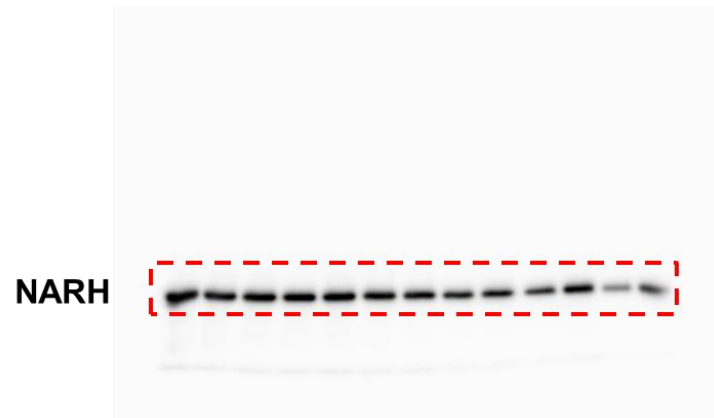


**Figure 5.** Target engagement of NARH assessed by CETSA.

**A**



**C**



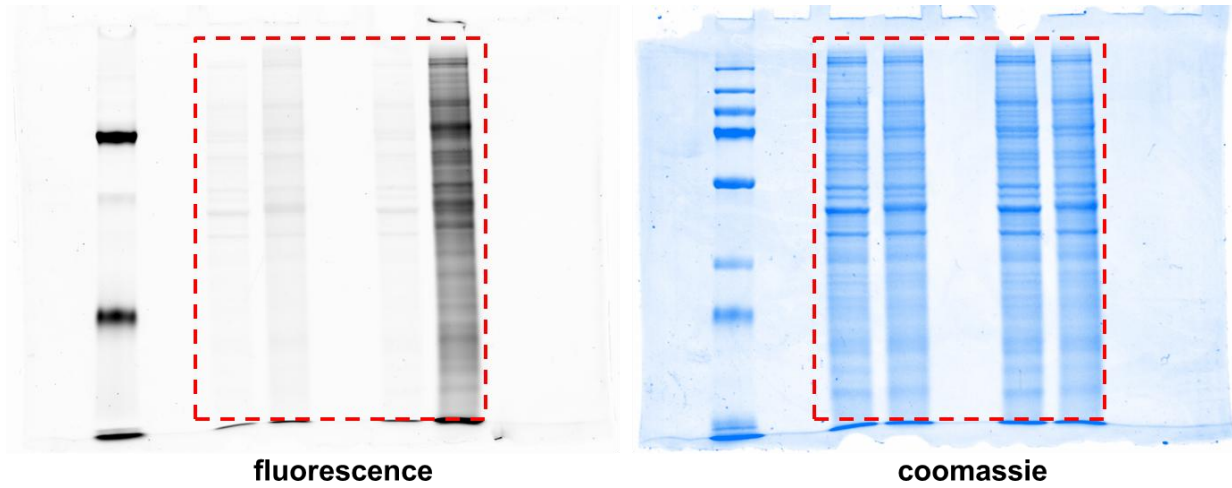
**E**





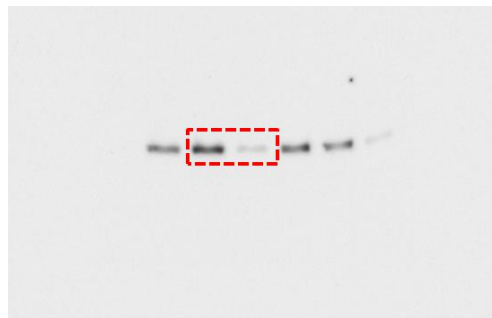
**Figure 6.** Activation of SIRT5 by NARH in cells.

**C**



**D**

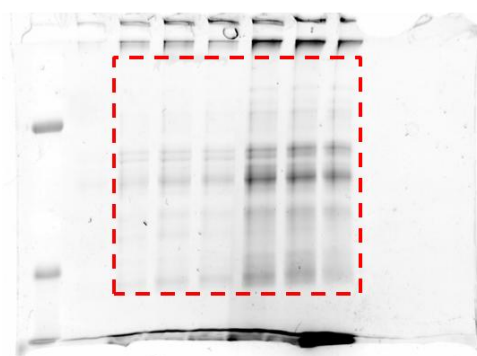
**SIRT5**



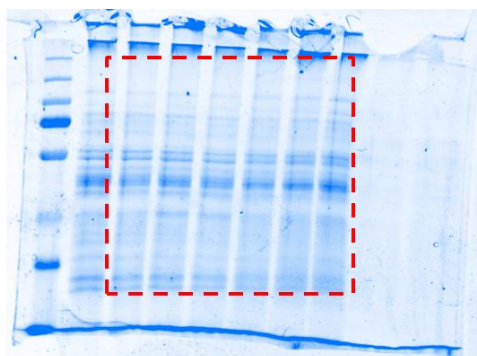
**$\alpha$ -tubulin**



**E**



**fluorescence**



**coomassie**

## REFERENCES

1. T. Yang, N. Y. Chan and A. A. Sauve, *J Med Chem*, 2007, **50**, 6458-6461.
2. N. Zhang and A. A. Sauve, *Curr Protoc Nucleic Acid Chem*, 2017, **71**, 14 14 11-14 14 19.
3. X. Bao, Q. Zhao, T. Yang, Y. M. Fung and X. D. Li, *Angew Chem Int Ed Engl*, 2013, **52**, 4883-4886.
4. A. Daina, O. Michielin and V. Zoete, *Sci Rep*, 2017, **7**, 42717.